Journal Pre-proofs

Detection of Novel RNA Viruses in wild Noble Crayfish (*Astacus astacus*): a Virome Analysis in Swiss water bodies

Tatiana Zingre, Simone Roberto Rolando Pisano, Nicole Wildi, Kara Lynne Dianne Dawson, Elodie Cristina, Torsten Seuberlich, Heike Schmidt-Posthaus

PII: S0022-2011(23)00128-3
DOI: https://doi.org/10.1016/j.jip.2023.108011
Reference: YJIPA 108011

To appear in: *Journal of Invertebrate Pathology*

Received Date: 7 August 2023
Revised Date: 24 October 2023
Accepted Date: 25 October 2023

Please cite this article as: Zingre, T., Roberto Rolando Pisano, S., Wildi, N., Lynne Dianne Dawson, K., Cristina, E., Seuberlich, T., Schmidt-Posthaus, H., Detection of Novel RNA Viruses in wild Noble Crayfish (*Astacus astacus*): a Virome Analysis in Swiss water bodies, *Journal of Invertebrate Pathology* (2023), doi: https://doi.org/10.1016/j.jip.2023.108011

Detection of Novel RNA Viruses in wild Noble Crayfish (*Astacus astacus*): a Virome Analysis in Swiss water bodies

Authors: Tatiana Zingre[a*], Simone Roberto Rolando Pisano[a*], Nicole Wildi[b], Kara Lynne Dianne Dawson[b], Elodie Cristina[a], Torsten Seuberlich[b], Heike Schmidt-Posthaus[a**]**

[a] Institute for Fish and Wildlife Health, Vetsuisse Faculty, University of Bern, Bern, Switzerland

[b] Division of Neurological Sciences, Vetsuisse Faculty, University of Bern, Bern, Switzerland

[*] Both authors have contributed equally to this work.

[**] Both authors have contributed equally to this work.

Highlights

- This study is the first virome analysis in noble crayfish (*Astacus astacus*).
- Bunya-like brown spot virus is a (-) ssRNA virus associated with a mass mortality event in white-clawed crayfish (*Austropotamobius pallipes*).
- We detected the near full-length genome of a closely related bunya-like virus in noble crayfish without associated mortality.
- Ten other RNA viruses (four hepe-like, two dicistro-like, three picorna-like, one permutotetra-like) were detected in the samples.

Abstract

European native crayfish populations are undergoing a strong decline due to environmental factors and the introduction of highly competitive non-native species. Pathogens are an

additional threat to native crayfish. However, aside from the crayfish plague, other infectious diseases are still widely unknown. This study aimed to investigate viruses present in seven populations of wild noble crayfish (*Astacus astacus*) in Switzerland, through high-throughput sequencing. Sequence analysis revealed the presence of 11 novel RNA viruses (one bunya-like, four hepe-like, two dicistro-like, three picorna-like, and one permutotetra-like) in the samples. The discovery of a novel bunya-like virus in noble crayfish without associated mortality or macroscopical alterations is of particular interest since it is closely related to the bunya-like brown spot virus, a virus described in 2019 from diseased native white-clawed crayfish (*Austropotamobius pallipes*) during a mass mortality event in France. It seems that these two closely related viruses have very different impacts on their respective hosts, raising the need for further investigations on virulence factors and host susceptibility towards these viruses. This study provides a basis for future investigations, permitting to gradually fill the knowledge gap in crayfish viral diseases.

Keywords

Crustacea; bunya-like virus; hepe-like virus; picorna-like virus; dicistro-like virus; permutotetra-like virus

1. Introduction

The noble crayfish (*Astacus astacus*), one of the three Swiss native species of crayfish, is listed as endangered in Switzerland (Ordonnance relative à la loi sur la pêche du 24 novembre 1993 (OLFP; RS 923.01) (Status as of 1st January 2021)) and as vulnerable at international level (Edsman et al., 2010). The decline of European crayfish is strongly related to the loss and degradation of aquatic environments and to competition with invasive non-native species, such as the signal crayfish (*Pacifastacus leniusculus*), the spinycheek crayfish (*Faxonius limosus*), and the red swamp crayfish (*Procambarus clarkii*) from North America as well as the narrow-clawed crayfish (*Pontastacus leptodactylus*) from Eastern Europe (Holdich et al., 2009). Along with the introduction of non-native species to a new region, there is a high risk of pathogen introduction, such as *Aphanomyces astaci*, the agent of the crayfish plague, which has been devastating to European crayfish populations since its introduction from North America (Foster et al., 2021; Martín-Torrijos et al., 2021). Although *A. astaci* is thought to be the main pathogen threatening wild European crayfish (Longshaw, 2011), additional infectious and non-infectious causes of death are rarely investigated. Further disease aetiologies in crayfish, such as viruses, should therefore be elucidated (Dragičević et al., 2021). For instance, the highly virulent white spot syndrome virus, which is listed as notifiable by the World Organisation for Animal Health (WOAH), causes devastating disease outbreaks in crustaceans (Sánchez-Martínez et al., 2007). Even if viral infections are not always highly pathogenic, they often weaken the hosts' immune system, making them more susceptible to secondary pathogenic agents or increasing disease prevalence and severity (Wang et al., 2019).

Recently, the use of metatranscriptomics, based on high-throughput sequencing (HTS) of tissue-extracted RNA and bioinformatics, has permitted to detect large numbers of viruses in crustaceans (Bačnik et al., 2021; Shi et al., 2016; Van Eynde et al., 2020), including a newly

described bunya-like virus (bunya-like brown spot virus, BBSV) associated with a mass-mortality event in European white-clawed crayfish (*Austropotamobius pallipes*) in France (Grandjean et al., 2019). Among the wide variety of viruses discovered by these methods, some are probable pathogens, although their relationship with their host and their relevance for health impairment remains unclear. It is thus important to explore the viral diversity and assess the virome of each crayfish species, in order to recognise potential emerging pathogens. Although the native noble crayfish is an endangered species, its virome is unknown and little is known about possible threatening viral diseases. The aim of this study was to investigate and compare the RNA virome in seven wild populations of noble crayfish in Switzerland using metatranscriptomics.

2. Material and methods

2.1. Ethical statement

The project followed the regulations of the Swiss Animal Welfare Act (SR 455) and Swiss Animal Welfare Ordinance (SR 455.1) with the license to perform animal experiments (National no. 35073, cantonal no. BE92/2022).

2.2. Sample collection

During a nationwide project on crayfish plague distribution and prevalence, seven populations of native noble crayfish (*Astacus astacus*) from four different Swiss cantons (St. Gallen (SG1-SG4), Thurgau (TG1), Solothurn (SO1) and Aargau (AG1), see figure S1) were sampled and sent to the Institute for Fish and Wildlife Health (FIWI, Bern, Switzerland) between June and October 2021. Upon arrival at the FIWI, animals (n=42) were euthanised using a chloroform overdose as described by Oidtmann et al. (2004) and subsequently dissected. For each crayfish, individual organ pools consisting of heart, gills, hepatopancreas, and green gland were sampled

in RNAlater (Merck & Cie, Buchs, Switzerland) and immediately frozen in liquid nitrogen. Samples were then stored at -80°C until RNA extraction.

2.3. RNA extraction and high-throughput sequencing (HTS)

Total RNA was extracted with the RNeasy Plus Mini Kit (Qiagen AG, Hombrechtikon, Switzerland), according to the manufacturer's instructions and stored at -80°C until further analysis. RNA extracts (n=42) were pooled per population (n=7) in equimolar amounts according to the RNA quantity. Following ribosomal depletion (RiboCop, Lexogen) and library preparation (Corall Total RNA-Seq Library Prep Kit, Lexogen), paired-end (2x150 bp) sequencing was performed on an Illumina NovaSeq 6000 with 10 Mio reads/animal.

2.4. Sequence analysis

HTS reads were quality checked using fastqc (version 0.11.7; https://www.bioinformatics.babraham.ac.uk/projects/fastqc/) and trimmed with fastp (v.0.12.5; Chen et al., 2018). Trimmed reads were assembled using SPAdes (v.3.12.0; Prjibelski et al., 2020). Assembled scaffolds were screened for homologs against the National Center for Biotechnology Information (NCBI) nonredundant protein sequence database using the blastx command in Basic Local Alignment Search Tool (BLAST; Camacho et al., 2009) and DIAMOND (v. 2.0.9; Buchfink et al., 2021), with a default e-value cut-off of 0.001. Sequences similar to bacteriophages or fungi-infecting viruses (*Narnaviridae*, *Mitoviridae*, *Totiviridae*, see supplementary Table S1) were excluded. In order to concentrate on virus candidates for which comprehensive and reliable sequence information was generated, scaffolds with blastx similarities to RNA virus proteins with a minimum length of 1000 nucleotides and a k-mer coverage >90 were chosen for further analysis. The k-mer coverage represents the number of reads containing a k-mer (calculated by the assembly software) and was used as a measure for scaffold abundancy.

Open reading frames (ORFs) in assembled scaffolds were predicted using Geneious Prime (v.11.0.18+10) and annotated manually using the Protein family (Pfam) database (Mistry et al., 2021)), the NCBI Conserved domain database (Lu et al., 2020), and palmID (https://github.com/ababaian/palmid). Pairwise amino acid identities between related sequences were obtained through sequence alignments performed with the Geneious Aligner with default settings. To complete the 5' terminus of the segments of the Astacus bunya-like virus 1, a rapid amplification of cDNA ends (RACE) was performed on each segment (5' RACE System for Rapid Amplification of cDNA Ends, version 2.0, Invitrogen) according to the manufacturer's instructions. The following seminested PCR was performed with the GoTaq Green Master Mix (Promega AG, Dübendorf, Switzerland) and provided Abridged Universal Amplification Primer (AUAP). Thermal cycling was conducted with 35 cycles at an annealing temperature of 55°C and 30 seconds elongation time. The 3' terminus was obtained with the same method, targeting the antigenomic viral RNA. Additionally, a one-step RT-PCR (New England Biolabs GmbH, Frankfurt am Main, Germany) with subsequent Sanger sequencing (Microsynth AG, Balgach, Switzerland) was performed on each segment of Astacus bunya-like virus 1 and on Astacus picorna-like virus 2 to resolve ambiguities in the sequences. The primers used in both methods are listed in the supplementary materials (Table S2). The schematic genome diagram in figure 1 was created in R 4.3.1 (R Core Team, 2023) with the circlize package (v.0.4.15; Gu et al., 2014). Read coverage was computed with BEDTools (Quinlan & Hall, 2010) and imported in R with the bedr package (v.1.0.4, https://cran.r-project.org/web/packages/bedr/index.html) and ggplot2 (v.3.4.3 Wickham et al., 2016)).

2.5. Phylogenetic analysis

To determine the phylogenetic position of Astacus hepe-like virus 1 to 4, a selection of blastx hits as well as representative members of the *Hepeviridae* were downloaded from the NCBI

database and multiple sequence alignments of the RNA-dependent RNA polymerase (RdRp) amino acid (aa) sequences were performed using MAFFT (v. 7.475; Katoh & Standley, 2013). The resulting alignment was analysed with iqtree (v.2.0.3; Nguyen et al., 2015) for the best fitting model, resulting in the Blosum62+F+R3 model (Henikoff & Henikoff, 1992). The tree was built under the maximum likelihood method with a bootstrap value set at 1000 and visualized in MEGA 11 (Tamura et al., 2021). For Astacus bunya-like virus 1, the RdRp, glycoprotein, and nucleocapsid aa sequences of representative members of the order *Bunyavirales* (inspired by Grandjean et al., 2019) were analysed as described above, with the following best fitting models: LG+F+R4 model (Le & Gascuel, 2008), PMB+F+R3 model (Veerassamy et al., 2003), and LG+G4 model (Le & Gascuel, 2008), respectively.

3. Results and Discussion

Raw reads ($3.8 \times 10^7 – 1.9 \times 10^8$ per library) could be assembled into a total of 326 virus-like sequences. Based on their length and k-mer coverage, 70 virus-like sequences were selected for further analysis. In one population (SG1), one scaffold that had fallen below cut-off was retrieved to obtain the missing sequence of a segmented genome (Astacus bunya-like virus 1, see section 3.1). The sequences in the resulting selection were assigned to 11 different novel viruses (Table 1) and will be described in the following sections.

3.1. Astacus bunya-like virus 1

Sixteen scaffolds with high k-mer coverage (90.6 to 7’237.5) were identified in five populations as closely related to the three segments (large (L), medium (M), and small (S)) of bunya-like brown spot virus (BBSV; Grandjean et al., 2019) with blastx identities ranging from 60.8% (S

segment) to 91.8% (L segment). The near full-length genome sequences were completed by 5'RACE-PCR using genomic and antigenomic viral RNA as templates.

The (-) ssRNA genome of Astacus bunya-like virus 1 is composed of three segments (L, M, S), each containing a single ORF (Fig. 1). The 5' terminus of each segment presents a conserved terminal sequence of 10 bases (…CAGUAACACA) at the 5' terminus. The 3' terminus consists of the reverse complementary terminal sequence, with a single nucleotide mismatch in segments L and S (Fig. 1, insets). Although the 3' terminus of the M segment could not be confirmed by PCR, the missing sequence is very likely UGUG… (reverse complementary to the …CACA at the 5' terminus) as for the other two segments. This terminal reverse complementarity creates pseudo-circular genome segments by non-covalent bonding of both termini (see insets in Fig.1). Note that the mismatch in segments L and S should not impede this bonding, also known as panhandle formation, and that such mismatches have also been observed in orthobunyaviruses (Barr & Wertz, 2005).

3.1.1. L segment

The L segment (6418 nucleotides, nt) contains a 6282 nt long ORF with an RNA-dependent RNA polymerase (RdRp) domain, as well as a N-terminal endonuclease motif, typical of members of the *Bunyaviridae* (Reguera et al., 2010). Compared to BBSV (MK881590), the 3' and 5' termini are longer by 44 and 477 nt, respectively (see alignment in supplementary figure S2). The coding sequence is 1078 nt longer than the incomplete ORF of BBSV with an aa identity of 88.3%. The pairwise identity between sequences of each investigated population is 100%.

Population	Blastx best hit	Length	Coverage	Id	Al	Proposed name
SG1	QCO84579.1_RNA-dependent_RNA_polymerase__partial_[Austropotamobius_brown_spot_virus]	1303	1741.0801	89.7	175	Astacus bunya-like virus 1, L
	QCO84580.1_glycoprotein__partial_[Austropotamobius_brown_spot_virus]	1266	3385.2164	84.3	421	Astacus bunya-like virus 1, M
	UKQ11003.1_polyprotein_[signal_crayfish_associated_hepe-like_virus_1]	10688	498.57068	49.3	1745	Astacus hepe-like virus 1
	UKQ11003.1_polyprotein_[signal_crayfish_associated_hepe-like_virus_1]	8113	280.46339	49.1	1747	Astacus hepe-like virus 2
	UKQ11004.1_hypothetical_protein_1_[signal_crayfish_associated_hepe-like_virus_1]	1487	2303.0119	74.5	458	Astacus hepe-like virus 3
	UKQ11036.1_hypothetical_protein__partial_[signal_crayfish_associated_picorna-like_virus_8]	4570	366.92204	66.7	201	Astacus picorna-like virus 3
	QCO84581.1_nucleocapsid_protein__partial_[Austropotamobius_brown_spot_virus]	811	7237.4762	87.7	122	Astacus bunya-like virus 1, S*
SG2	QCO84579.1_RNA-dependent_RNA_polymerase__partial_[Austropotamobius_brown_spot_virus]	6469	858.06174	86.1	966	Astacus bunya-like virus 1, L
	QCO84580.1_glycoprotein__partial_[Austropotamobius_brown_spot_virus]	2925	1113.9146	82.9	573	Astacus bunya-like virus 1, M
	QCO84581.1_nucleocapsid_protein__partial_[Austropotamobius_brown_spot_virus]	1307	2702.6262	60.8	227	Astacus bunya-like virus 1, S
	UKQ11003.1_polyprotein_[signal_crayfish_associated_hepe-like_virus_1]	10468	428.35004	48.9	1747	Astacus hepe-like virus 3
	UNY42000.1_MAG:_polyprotein_1_[Picornavirales_sp.]	9200	225.65325	33.8	1561	Astacus dicistro-like virus 1
	APG76944.1_RdRp__partial_[Beihai_permutotetra-like_virus_1]	5038	425.5294	34.2	1004	Astacus permutotetra-like virus 1
SG3	QCO84579.1_RNA-dependent_RNA_polymerase__partial_[Austropotamobius_brown_spot_virus]	6293	612.51074	90.7	1117	Astacus bunya-like virus 1, L
	QCO84580.1_glycoprotein__partial_[Austropotamobius_brown_spot_virus]	2925	838.56481	82.4	506	Astacus bunya-like virus 1, M
	QCO84581.1_nucleocapsid_protein__partial_[Austropotamobius_brown_spot_virus]	1294	1226.5908	76.5	251	Astacus bunya-like virus 1, S
	UKQ11003.1_polyprotein_[signal_crayfish_associated_hepe-like_virus_1]	2221	1423.0065	62.7	619	Astacus hepe-like virus 2
	UKQ11003.1_polyprotein_[signal_crayfish_associated_hepe-like_virus_1]	8204	244.90833	49	1731	Astacus hepe-like virus 3
	UNY42000.1_MAG:_polyprotein_1_[Picornavirales_sp.]	9200	130.86736	33.8	1561	Astacus dicistro-like virus 1
	DAZ87488.1_TPA_asm:_capsid_protein_precursor_[Strongylocentrotus_intermedius_associated_picornavirus_1]	3375	216.17108	31.2	843	Astacus dicistro-like virus 2
SG4	UKQ11006.1_hypothetical_protein_3_[signal_crayfish_associated_hepe-like_virus_1]	1566	697.72733	47.4	306	Astacus hepe-like virus 2
	UKQ11003.1_polyprotein_[signal_crayfish_associated_hepe-like_virus_1]	8174	91.543663	48.8	1742	Astacus hepe-like virus 3
	UNY42000.1_MAG:_polyprotein_1_[Picornavirales_sp.]	9150	109.32271	33.8	1561	Astacus dicistro-like virus 1
TG1	QCO84579.1_RNA-dependent_RNA_polymerase__partial_[Austropotamobius_brown_spot_virus]	6469	90.570159	88.8	1703	Astacus bunya-like virus 1, L
	QCO84580.1_glycoprotein__partial_[Austropotamobius_brown_spot_virus]	2867	171.27667	85.3	916	Astacus bunya-like virus 1, M
	QCO84581.1_nucleocapsid_protein__partial_[Austropotamobius_brown_spot_virus]	1331	701.4185	65.9	343	Astacus bunya-like virus 1, S
	UKQ11003.1_polyprotein_[signal_crayfish_associated_hepe-like_virus_1]	10724	122.75949	49.3	1745	Astacus hepe-like virus 1
	UKQ11003.1_polyprotein_[signal_crayfish_associated_hepe-like_virus_1]	2611	1525.4358	57.6	632	Astacus hepe-like virus 2
	UKQ11003.1_polyprotein_[signal_crayfish_associated_hepe-like_virus_1]	11574	130.78297	49	1762	Astacus hepe-like virus 4
SO1	UKQ11006.1_hypothetical_protein_3_[signal_crayfish_associated_hepe-like_virus_1]	1266	8425.6639	43.3	97	Astacus hepe-like virus 2
	UKQ11003.1_polyprotein_[signal_crayfish_associated_hepe-like_virus_1]	6040	857.67686	41.5	1258	Astacus hepe-like virus 3
	QYV43043.1_MAG:_polyprotein_[Picornavirales_sp.]	9700	1031.473	22.4	814	Astacus picorna-like virus 2
	DAZ87869.1_TPA_asm:_hypothetical_protein_[Dugejap_virus_1]	8722	253.30807	31.2	1680	Astacus picorna-like virus 1
AG1	QCO84581.1_nucleocapsid_protein__partial_[Austropotamobius_brown_spot_virus]	1307	4563.6038	81.7	218	Astacus bunya-like virus 1, S
	QCO84579.1_RNA-dependent_RNA_polymerase__partial_[Austropotamobius_brown_spot_virus]	3257	3054.5144	87.8	1085	Astacus bunya-like virus 1, L
	QCO84580.1_glycoprotein__partial_[Austropotamobius_brown_spot_virus]	2984	1602.0864	85.4	916	Astacus bunya-like virus 1, M

Table 1 Selected viruses present in seven populations of noble crayfish (*Astacus astacus*) in Switzerland. The best hit in the blastx analysis is indicated, with the protein sequence identity (Id [%]) and protein alignment length (Al, in nucleotides). The scaffold length (in nucleotides) and k-mer coverage are also given. Note that in population SG1, one scaffold below the set cut-off (length=1kb, k-mer coverage=90) is included in this compilation (*).

3.1.2. M segment

The M segment (2870 nt) contains a 2727 nt long ORF with glycoprotein domains (G1, G2 fusion, and G2 C-terminal). Note that the predicted ORF begins with a start codon that is located in the conserved decamer sequence, at position 2 (resp. position 6 with the four missing nucleotides) but is probably non-functional. The putative functional start codon is found at position 32 (resp. position 36). The 3' and 5' termini are longer than those of BBSV (MK881591) by 5 and 25 nt, respectively (see Fig. S2). The predicted ORF has an aa identity of 86% with BBSV and 98.4% to 100% between each investigated population.

3.1.3. S segment

The S segment (1256 nt) has one ORF (1014 nt) encoding for a protein with a nucleocapsid protein domain. The 3' terminus is 29 nt longer than in BBSV (MK881592), and the 5' terminus is 19 nt shorter (see Fig. S2). Since Grandjean et al. (2019) did not obtain the full genome of BBSV, their annotated coding sequence continues upstream of the first AUG in the sequence (position 19). However, the alignment with Astacus bunya-like virus 1 permits to argue that the AUG on position 19 (respectively position 48 on our sequence) is the correct start codon. The ORF has a 66.2% aa identity with BBSV, and all investigated populations have a 100% aa identity between each other.

3.1.4. Phylogenetic relationships

Phylogenetic analysis of all segments of Astacus bunya-like virus 1 indicates its inclusion in the family *Phenuiviridae* and its close relationship to BBSV. Both viruses are placed as sister groups in a clade containing Wenling crustacean virus 7 and otter fecal bunyavirus, as observed by Grandejan et al. (2019) (see Fig. 2, and supplementary figures S3 and S4). Despite their close relationship, Astacus bunya-like virus 1 and BBSV most likely represent different crayfish-infecting viruses. The aa identities of the L and M segments between Astacus bunya-like virus 1 and BBSV are relatively high (88.3% and 86%, respectively). Such high identity

levels are not surprising for the L segment, as it encodes the highly conserved RdRp. Similarly, the M segment of two closely related crayfish-infecting viruses can be expected to share such a high aa identity, as glycoproteins are important for cell entry (Hulswit et al., 2021). On the other hand, the aa identity of the S segment is comparatively low (only 66.2%). It has, however, been described that the nucleoprotein presents limited similarities between genera and families (Ter Horst et al., 2019).

The conserved terminal decamer sequence (…CAG***U***AACACA) present at the 5' terminus of each segment seems to further support the phylogenetic position of Astacus bunya-like virus 1. It is indeed very similar to that of phleboviruses (Type species: *Phlebovirus riftense*) and of oriental wenrivirus 1 (…CAG***A***AACACA) (Dong et al., 2021; King et al., 2012a). Unfortunately, the terminal sequences have not been yet determined for any of the closer relatives (e.g., BBSV, Wenling crustacean virus 7, otter fecal bunyavirus or Hubei bunya-like virus 1) and it is thus not possible at the moment to know whether the nucleotide difference (U instead of A) is found in a particular clade.

Additionally, the decamer sequence at the 3' termini of segments L and S of Astacus bunya-like virus 1 have one nucleotide mismatch compared to the 5' sequence at position 6 and 7, respectively. It would be interesting to know whether other closely related crayfish-associated bunya-like viruses also present these mismatches. To date, there are however only two other known bunya-like viruses in crayfish: athtab bunya-like virus (Sakuna et al., 2018) and BBSV (Grandjean et al., 2019). Athtab bunya-like virus is described as closely related to members of the *Peribunyaviridae* family and is thus phylogenetically distant to BBSV and Astacus bunya-like virus 1. For BBSV, the genome termini remain undetermined for now and can therefore not be compared.

3.1.5. Relevance

Despite their close phylogenetic relationship, Astacus bunya-like virus 1 and BBSV do not seem to produce the same pathology on their putative hosts. BBSV was described from a mass mortality event of *A. pallipes,* where diseased individuals presented distinctive brown discolorations on their cuticle (Grandjean et al., 2019). Although it could not be definitively established, investigations suggest a causal association between the mortality event and the BBSV infection. All crayfish with clinical signs (sampled from the mortality event and with brown spots on their cuticle) were tested positive for viral presence by PCR and subsequent Sanger sequencing, whereas apparently healthy crayfish (sampled from unaffected locations and without brown spots on the cuticle) tested negative. Additionally, transmission electron microscopy of tissues (muscle, nerve chain, hepatopancreas) from two infected crayfish revealed viral particles morphologically similar to phleboviruses, which were absent in the samples of non-infected individuals. Finally, despite the initial suspicion of a crayfish plague outbreak, all investigated crayfish tested negative for the presence of *A. astaci*. In the present study, however, none of the *A. astacus* analysed had brown discolorations on their cuticle. Furthermore, only one of the five populations (SO1) associated with Astacus bunya-like virus 1 experienced mortality, which was probably due to an outbreak of crayfish plague since *A. astaci* DNA was detected during an ongoing research project (Pisano, unpublished results).

It is possible that Astacus bunya-like virus 1 is better adapted to *A. astacus* (and vice versa) since pathology or mortality do not seem to be associated with this virus infection to date. It would thus be important to investigate if pathology and lethality in BBSV infections are related to specific virulence factors, or rather to the host's susceptibility, including aggravating factors such as water quality or other co-infections.

Other Swiss crayfish species, including white-clawed crayfish, should also be analysed to determine if they are infected by bunya-like viruses and, if that is the case, to assess their

phylogenetic relations with currently known viruses, potentially revealing a common origin and elucidating their role for crayfish health.

3.2. Astacus hepe-like virus 1-4

Out of the seven crayfish populations, six had viral-like contigs similar to signal crayfish-associated hepe-like virus 1, a virus described from a metagenomic study of Croatian signal crayfish (Bačnik et al., 2021). Four near full-length genomes could be distinguished and were present with high k-mer coverage (ranging from 91.5 to 9383.4). All are organised into five ORFs, with an overlap between ORF 1 and 2 (10 nt for Astacus hepe-like virus 1 and 4, 16 nt for Astacus hepe-like virus 2 and 3). To correctly assign all sub-genomic sequences to Astacus hepe-like virus 2, and to confirm the presence of ORF 4 and 5, a sequence that had fallen below cut-off had to be retrieved (Node 23, 9923 nt, k-mer coverage 36.3), also revealing a poly-A tail at the 3' end. This polyadenylation is also present in Astacus hepe-like virus 3, and in a sequence below cut-off (coverage=77.4) of Astacus hepe-like virus 1. The two first ORFs contain motifs for methyltransferase (ORF1), helicase (ORF1), and RNA-dependent RNA polymerase (ORF2) (Fig. 3), which are usually found in one single ORF in the *Hepeviridae* family (Purdy et al., 2022). The second ORF in members of the *Hepeviridae* encodes for capsid proteins, which should be located in at least one of the remaining three ORFs of Astacus hepe-like virus 1-4, but no clear motif resembling capsid-like proteins could be found.

The genomic organisation of the four novel viruses is consistent with that of signal crayfish hepe-like virus 1. The presence of the fifth, shorter ORF, is not reported by Bačnik et al. (2021) but can be found in the submitted sequence (OK317707). Moreover, it is consistent with the sequence of another related virus, the Beihai hepe-like virus 4, as well as other hepe-like viruses isolated from aquatic organisms (Shi et al., 2016). Overall, the four viruses are clearly distinct

from signal crayfish-associated hepe-like virus (see aa identities of each ORF with respect to reference in Fig. 3), but still form a phylogenetic cluster (Fig. 4). Astacus hepe-like virus 2 and 3 are very similar, with aa identities for proteins encoded by ORF 2, 3 and 4 ranging from 96.7% to 98.0%. The identity of the proteins encoded by ORF 1 is, however, lower (86.7%). Taken together with the overall sequence divergence (19.3% at the nucleotide level), we conclude that Astacus hepe-like virus 2 and 3 are different viral strains. A table with pairwise identities between each of the four viruses can be found in the supplementary material (Fig. S5).

Hepe-like viruses in crustaceans have mostly been identified through metagenomic studies, and very little is known about their relevance (Bačnik et al., 2021; Shi et al., 2016; Van Eynde et al., 2020). Except for Crustacea hepe-like virus 1, which was isolated from giant freshwater prawn (*Macrobrachium rosenbergii*) with growth retardation (Dong et al., 2020), there have been no reports yet that hepe-like viruses might be pathogenic to crustaceans. In the present study, Astacus hepe-like virus 4 is the only virus that was found solely in a population with mortality (TG1), where *A. astaci* DNA was not detected. This is interesting, as it shows slight differences in genome organisation with the other three viruses, and stands out in the phylogenetical analysis (see Figs. 3 and 4). Although no claim about its pathogenicity can be made on this basis, further investigations are necessary to elucidate whether a significant difference can be found with the other Astacus hepe-like viruses, potentially indicating the presence of virulence factors.

3.3. Picornavirales

Five different scaffolds with similarities to viruses in the order *Picornavirales* were detected. Viral candidates with genome organisation similar to the family *Dicistroviridae* were

tentatively named “dicistro-like” viruses and candidates which could not be clearly assigned to a family were named “picorna-like” viruses.

Astacus dicistro-like virus 1 was found in three populations with an average k-mer coverage of 155.3. The scaffold has a length of 9200 nucleotides and is organised into two non-overlapping ORFs and a poly-A tail at the 3’ end. The best match in the blastx analysis was the RdRp of a member of the *Picornaviridae* family found in a Chinese environmental RNA study (Y.-M. Chen et al., 2022), with a blastx identity of 33.8%. The genome organisation, however, coincides with that of the *Dicistroviridae:* 8-10 kilobases (kb; present virus: 9.2 kb), GC content ranging from 34% to 45% (present virus: 40.2%), two ORFs of approximately 5’500 nt (present virus: 5’463 nt) and 2’700 nt (present virus: 2’508 nt), that are separated by an intergenic untranslated region of 170–530 nt (present virus: 371 nt), and a polyadenylated 3’ terminus (Valles et al., 2017).

Astacus dicistro-like virus 2 is represented by a partial sequence of 3375 nt and reveals an ORF encoding for a protein with capsid protein motifs and with 35.1% blastx identity with the hypothetical protein 2 of Beihai picorna-like virus 70. It has a sequence identity of 78 % with Astacus dicistro-like virus 1 and a 93.7% aa identity with the protein encoded by its ORF 2.

These viruses could be of interest for crustacean health, as the *Dicistroviridae* family comprises pathogenic viruses, including Taura syndrome virus (*Aparavirus tauraense*), a WOAH-notifiable virus of high relevance in the penaeid shrimp industry (Stentiford et al., 2009). Although Astacus dicistro-like virus 1 and 2 were found in three apparently healthy populations without associated mortality, the current state of knowledge does not permit to exclude pathogenicity, and further investigations would be required to gain a better understanding of the role of dicistro-like viruses in crayfish.

Astacus picorna-like virus 1, is represented by a sequence with a partial ORF (8722 nt) which encodes for a protein that reveals different motifs (helicase, 3c cysteine protease, RdRp, capsid-

like proteins) and a poly-A tail at the 3' end. It was only found in one population (SO1). The best match in the blastx analysis (33.1 %) was, as for Astacus dicistro-like virus 1, the RdRp of a member of the *Picornaviridae* (Y.-M. Chen et al., 2022), and other blastx matches also include dicistroviruses. However, with the presence of one single ORF, the genome structure does not correspond to that of the *Dicistroviridae*.

Astacus picorna-like virus 2 is represented by the longest contig (9781 nt) and is organised in one single ORF encoding for a protein with helicase and RdRp motifs. It has a 35.2% blastx identity with the Wenzhou shrimp virus 8, Penaeus vannamei solinivirus and Penaeus vannamei picornavirus, three highly similar viruses submitted separately with different names.

Astacus picorna-like virus 3, 4750 nt, contains one predicted ORF (encoding for a protein that reveals a helicase motif, but interestingly, no RdRp motif), and a poly-A tail at the 3' end. The protein shows an aa similarity of 66.7% with that from signal crayfish associated picorna-like virus 8 (partial sequence of 734 nt, OK317729).

Other than in the family *Dicistroviridae*, few members of the *Picornavirales* order are known to be pathogenic to crustaceans. In crayfish, two viruses have been described from Australia, Cherax albidus picorna-like virus (CaPV or "Yabby virus") and chequa iflavirus (Jones & Lawrence, 2001; Sakuna et al., 2017). CaPV was associated with mortalities in white yabbies (*Cherax albidus*), but there have not been further reports since 2001. Chequa iflavirus was discovered in stressed redclaw crayfish (*Cherax quadricarinatus*) in 2017 but is probably not the cause of mortalities and might even be a virus present since the 1990s, without any disease development (Sakuna et al., 2017). A recent review on crustacean viral diseases only cites three other putative *Picornaviridae*, described in the 1970s (Bateman & Stentiford, 2017). These viruses have, however, only been described morphologically (and are thus indistinguishable from dicistroviruses) and would require further characterisation.

3.4. Astacus permutotetra-like virus 1

One sequence found in a population (SG2) without apparent clinical disease consists of 5038 nt, organised into one main ORF (4728 nt) and one potential smaller overlapping ORF (1842 nt). This sequence matched with Beihai permutotetra-like virus 1, a virus described from a large metatranscriptomic study of invertebrates (Shi et al., 2016), with low aa identity (32.5%).

The *Permutotetraviridae* is a family of (+) ssRNA viruses that were until recently believed to only infect lepidopterans (King et al., 2012b). However, recent studies indicate the presence of permutotetra-like viruses in other arthropods, including crustaceans (Ribeiro et al., 2020; Shi et al., 2016). The effect of these viruses on their hosts is still unknown, but in Lepidoptera, infections range from asymptomatic to highly lethal and mostly affect larval stages (Hanzlik & Gordon, 1997).

4. Conclusion

This study permits a first glance in the virome of noble crayfish and of Swiss crayfish in general, significantly increasing the scarce knowledge on viral diversity in crayfish and providing a framework for future studies on native and invasive species. We detected 11 novel RNA viruses in seven Swiss noble crayfish populations, one bunya-like virus, four hepe-like viruses, two dicistro-like viruses, three picorna-like viruses, and one permutotetra-like virus. Moreover, we were able to obtain the near full-length genome of the Astacus bunya-like virus 1 and to compare it with a closely related virus, the bunya-like brown spot virus, which has been associated with mass mortality events in white-clawed crayfish in France. Although this study did not permit to associate virus detection with pathogenicity and mortality, the identified viruses require awareness as their impact on crayfish health still needs to be elucidated. Therefore, further investigations including a more comprehensive sampling of Swiss noble crayfish populations, as well as other native and invasive species are indicated to expand the

knowledge on the geographical distribution of each virus and their regional and species-specific strains. A comparison between similar viruses could also permit to elucidate their origin, potential host adaptation, and pathogenicity. By comparing healthy and diseased crayfish, the viral infections should be better characterised, to determine if they are asymptomatic, symptomatic on their own, or exacerbating other co-infections, such as the crayfish plague. This is especially important for endangered native European species undergoing massive population decline, as we need to increase our knowledge on any potential threat to their fragile conservation.

Data availability

Raw data has been deposited in the European Nucleotide Archive at EMBL-EBI under project PRJEB62779 (https://www.ebi.ac.uk/ena/browser/view/PRJEB62779), where populations are named as follows: F21/207 (SG1), F21/208 (SG2), F21/210 (SG3), F21/211 (SG4), F21/347 (TG1), F21/367 (SO1), Farm (AG1). The sequences to the eleven viruses described in this study are available under accession numbers OY734085, OY742858-OY742865, OY746346, OY746347, OY746349 and OY746350.

Acknowledgments

We would like to thank the fish wardens, fishery inspectors, and private persons of the cantons Aargau, St. Gallen, Solothurn, and Thurgau for providing the wild crayfish. We also thank the FIWI team for their help in sampling, Pamela Nicholson and the NGS Platform team (University of Bern, Switzerland) for performing the sequencing, and Simone Oberhänsli for sequence submission. We are also grateful to Gary Delalay for producing Figure 1, Pia Cigler for drawing the noble crayfish used in Figs. 4 and S1 as well as in the graphical abstract, and Vivien Cosandey for providing improvements to the manuscript. Figures 3 and icons in Figure 4 were created with BioRender.com.

References

Bačnik, K., Kutnjak, D., Černi, S., Bielen, A., & Hudina, S. (2021). Virome Analysis of Signal Crayfish (*Pacifastacus leniusculus*) along Its Invasion Range Reveals Diverse and Divergent RNA Viruses. *Viruses*, *13*(11), 2259. https://doi.org/10.3390/v13112259

Barr, J. N., & Wertz, G. W. (2005). Role of the Conserved Nucleotide Mismatch within 3′- and 5′-Terminal Regions of Bunyamwera Virus in Signaling Transcription. *Journal of Virology*, *79*(6), 3586‑3594. https://doi.org/10.1128/JVI.79.6.3586-3594.2005

Bateman, K. S., & Stentiford, G. D. (2017). A taxonomic review of viruses infecting crustaceans with an emphasis on wild hosts. *Journal of Invertebrate Pathology*, *147*, 86‑110. https://doi.org/10.1016/j.jip.2017.01.010

Buchfink, B., Reuter, K., & Drost, H.-G. (2021). Sensitive protein alignments at tree-of-life scale using DIAMOND. *Nature Methods*, *18*(4), Article 4. https://doi.org/10.1038/s41592-021-01101-x

Camacho, C., Coulouris, G., Avagyan, V., Ma, N., Papadopoulos, J., Bealer, K., & Madden, T. L. (2009). BLAST+ : Architecture and applications. *BMC Bioinformatics*, *10*(1), 421. https://doi.org/10.1186/1471-2105-10-421

Chen, S., Zhou, Y., Chen, Y., & Gu, J. (2018). fastp : An ultra-fast all-in-one FASTQ preprocessor. *Bioinformatics*, *34*(17), i884‑i890. https://doi.org/10.1093/bioinformatics/bty560

Chen, Y.-M., Sadiq, S., Tian, J.-H., Chen, X., Lin, X.-D., Shen, J.-J., Chen, H., Hao, Z.-Y., Wille, M., Zhou, Z.-C., Wu, J., Li, F., Wang, H.-W., Yang, W.-D., Xu, Q.-Y., Wang, W., Gao, W.-H., Holmes, E. C., & Zhang, Y.-Z. (2022). RNA viromes from terrestrial sites across China expand environmental viral diversity. *Nature Microbiology*, *7*(8), Article 8. https://doi.org/10.1038/s41564-022-01180-2

Dong, X., Hu, T., Liu, Q., Li, C., Sun, Y., Wang, Y., Shi, W., Zhao, Q., & Huang, J. (2020). A Novel Hepe-Like Virus from Farmed Giant Freshwater Prawn *Macrobrachium rosenbergii*. *Viruses*, *12*(3). https://doi.org/10.3390/v12030323

Dong, X., Hu, T., Ren, Y., Meng, F., Li, C., Zhang, Q., Chen, J., Song, J., Wang, R., Shi, M., Li, J., Zhao, P., Li, C., Tang, K. F. J., Cowley, J. A., Shi, W., & Huang, J. (2021). A Novel Bunyavirus Discovered in Oriental Shrimp (*Penaeus chinensis*). *Frontiers in Microbiology*, *12*, 751112. https://doi.org/10.3389/fmicb.2021.751112

Dragičević, P., Bielen, A., Petrić, I., & Hudina, S. (2021). Microbial pathogens of freshwater crayfish : A critical review and systematization of the existing data with directions for future research. *Journal of Fish Diseases*, *44*(3), 221‑247. https://doi.org/10.1111/jfd.13314

Edsman, L., Füreder, L., Gherardi, F., & Souty-Grosset, C. (2010). IUCN Red List of Threatened Species : *Astacus astacus*. *IUCN Red List of Threatened Species*. https://www.iucnredlist.org/en

Foster, R., Peeler, E., Bojko, J., Clark, P. F., Morritt, D., Roy, H. E., Stebbing, P., Tidbury, H. J., Wood, L. E., & Bass, D. (2021). Pathogens co-transported with invasive non-native aquatic species : Implications for risk analysis and legislation. *NeoBiota*, *69*, 79‑102. https://doi.org/10.3897/neobiota.69.71358

Grandjean, F., Gilbert, C., Razafimafondy, F., Vucić, M., Delaunay, C., Gindre, P., Bouchard, J., Raimond, M., & Moumen, B. (2019). A new bunya-like virus associated with mass mortality of white-clawed crayfish in the wild. *Virology*, *533*, 115‑124. https://doi.org/10.1016/j.virol.2019.05.014

Gu, Z., Gu, L., Eils, R., Schlesner, M., & Brors, B. (2014). Circlize Implements and enhances circular visualization in R. *Bioinformatics (Oxford, England)*, *30*(19), 2811‑2812. https://doi.org/10.1093/bioinformatics/btu393

Hanzlik, T. N., & Gordon, K. H. J. (1997). The Tetraviridae. In K. Maramorosch, F. A. Murphy, & A. J. Shatkin (Éds.), *Advances in Virus Research* (Vol. 48, p. 101‑168). Academic Press. https://doi.org/10.1016/S0065-3527(08)60287-0

Henikoff, S., & Henikoff, J. G. (1992). Amino acid substitution matrices from protein blocks. *Proceedings of the National Academy of Sciences*, *89*(22), 10915‑10919. https://doi.org/10.1073/pnas.89.22.10915

Holdich, D. M., Reynolds, J. D., Souty-Grosset, C., & Sibley, P. J. (2009). A review of the ever increasing threat to European crayfish from non-indigenous crayfish species. *Knowledge and Management of Aquatic Ecosystems*, *394‑395*, Article 394‑395. https://doi.org/10.1051/kmae/2009025

Hulswit, R. J. G., Paesen, G. C., Bowden, T. A., & Shi, X. (2021). Recent Advances in Bunyavirus Glycoprotein Research : Precursor Processing, Receptor Binding and Structure. *Viruses*, *13*(2), 353. https://doi.org/10.3390/v13020353

Jones, J. B., & Lawrence, C. S. (2001). Diseases of yabbies (*Cherax albidus*) in Western Australia. *Aquaculture*, *194*(3), 221‑232. https://doi.org/10.1016/S0044-8486(00)00508-1

Katoh, K., & Standley, D. M. (2013). MAFFT Multiple Sequence Alignment Software Version 7 : Improvements in Performance and Usability. *Molecular Biology and Evolution*, *30*(4), 772‑780. https://doi.org/10.1093/molbev/mst010

King, A. M. Q., Adams, M. J., Carstens, E. B., & Lefkowitz, E. J. (Éds.). (2012a). Family—*Bunyaviridae*. In *Virus Taxonomy* (p. 725‑741). Elsevier. https://doi.org/10.1016/B978-0-12-384684-6.00059-8

King, A. M. Q., Adams, M. J., Carstens, E. B., & Lefkowitz, E. J. (Éds.). (2012b). Family—*Tetraviridae*. In *Virus Taxonomy* (p. 1091‑1102). Elsevier. https://doi.org/10.1016/B978-0-12-384684-6.00094-X

Le, S. Q., & Gascuel, O. (2008). An improved general amino acid replacement matrix. *Molecular Biology and Evolution*, *25*(7), 1307‑1320. https://doi.org/10.1093/molbev/msn067

Longshaw, M. (2011). Diseases of crayfish : A review. *Journal of Invertebrate Pathology*, *106*(1), 54‑70. https://doi.org/10.1016/j.jip.2010.09.013

Lu, S., Wang, J., Chitsaz, F., Derbyshire, M. K., Geer, R. C., Gonzales, N. R., Gwadz, M., Hurwitz, D. I., Marchler, G. H., Song, J. S., Thanki, N., Yamashita, R. A., Yang, M., Zhang, D., Zheng, C., Lanczycki, C. J., & Marchler-Bauer, A. (2020). CDD/SPARCLE : The conserved domain database in 2020. *Nucleic Acids Research*, *48*(D1), D265‑D268. https://doi.org/10.1093/nar/gkz991

Martín-Torrijos, L., Martínez-Ríos, M., Casabella-Herrero, G., Adams, S. B., Jackson, C. R., & Diéguez-Uribeondo, J. (2021). Tracing the origin of the crayfish plague pathogen, Aphanomyces astaci, to the Southeastern United States. *Scientific Reports*, *11*(1), Article 1. https://doi.org/10.1038/s41598-021-88704-8

Mistry, J., Chuguransky, S., Williams, L., Qureshi, M., Salazar, G. A., Sonnhammer, E. L. L., Tosatto, S. C. E., Paladin, L., Raj, S., Richardson, L. J., Finn, R. D., & Bateman, A. (2021). Pfam : The protein families database in 2021. *Nucleic Acids Research*, *49*(D1), D412‑D419. https://doi.org/10.1093/nar/gkaa913

Nguyen, L.-T., Schmidt, H. A., von Haeseler, A., & Minh, B. Q. (2015). IQ-TREE : A Fast and Effective Stochastic Algorithm for Estimating Maximum-Likelihood Phylogenies. *Molecular Biology and Evolution*, *32*(1), 268‑274. https://doi.org/10.1093/molbev/msu300

Oidtmann, B., Schaefers, N., Cerenius, L., Söderhäll, K., & Hoffmann, R. W. (2004). Detection of genomic DNA of the crayfish plague fungus *Aphanomyces astaci* (Oomycete) in clinical samples by PCR. *Veterinary Microbiology*, *100*(3), 269‑282. https://doi.org/10.1016/j.vetmic.2004.01.019

Prjibelski, A., Antipov, D., Meleshko, D., Lapidus, A., & Korobeynikov, A. (2020). Using SPAdes De Novo Assembler. *Current Protocols in Bioinformatics*, *70*(1), e102. https://doi.org/10.1002/cpbi.102

Purdy, M. A., Drexler, J. F., Meng, X.-J., Norder, H., Okamoto, H., Van der Poel, W. H. M., Reuter, G., de Souza, W. M., Ulrich, R. G., & Smith, D. B. (2022). ICTV Virus Taxonomy Profile : *Hepeviridae* 2022. *Journal of General Virology*, *103*(9), 001778. https://doi.org/10.1099/jgv.0.001778

Quinlan, A. R., & Hall, I. M. (2010). BEDTools : A flexible suite of utilities for comparing genomic features. *Bioinformatics*, *26*(6), 841‑842. https://doi.org/10.1093/bioinformatics/btq033

Reguera, J., Weber, F., & Cusack, S. (2010). *Bunyaviridae* RNA polymerases (L-protein) have an N-terminal, influenza-like endonuclease domain, essential for viral cap-dependent transcription. *PLoS Pathogens*, *6*(9), e1001101. https://doi.org/10.1371/journal.ppat.1001101

Ribeiro, G. de O., Morais, V. S., Monteiro, F. J. C., Ribeiro, E. S. D., Rego, M. O. da S., Souto, R. N. P., Villanova, F., Tahmasebi, R., Hefford, P. M., Deng, X., Delwart, E., Cerdeira

Sabino, E., Fernandes, L. N., da Costa, A. C., & Leal, É. (2020). *Aedes aegypti* from Amazon Basin Harbor High Diversity of Novel Viral Species. *Viruses*, *12*(8), 866. https://doi.org/10.3390/v12080866

Sakuna, K., Elliman, J., & Owens, L. (2017). Discovery of a novel *Picornavirales*, Chequa iflavirus, from stressed redclaw crayfish (*Cherax quadricarinatus*) from farms in northern Queensland, Australia. *Virus Research*, *238*, 148‑155. https://doi.org/10.1016/j.virusres.2017.06.021

Sakuna, K., Elliman, J., Tzamouzaki, A., & Owens, L. (2018). A novel virus (order *Bunyavirales*) from stressed redclaw crayfish (*Cherax quadricarinatus*) from farms in northern Australia. *Virus Research*, *250*, 7‑12. https://doi.org/10.1016/j.virusres.2018.03.012

Sánchez-Martínez, J. G., Aguirre-Guzmán, G., & Mejía-Ruíz, H. (2007). White Spot Syndrome Virus in cultured shrimp : A review. *Aquaculture Research*, *38*(13), 1339‑1354. https://doi.org/10.1111/j.1365-2109.2007.01827.x

Shi, M., Lin, X.-D., Tian, J.-H., Chen, L.-J., Chen, X., Li, C.-X., Qin, X.-C., Li, J., Cao, J.-P., Eden, J.-S., Buchmann, J., Wang, W., Xu, J., Holmes, E. C., & Zhang, Y.-Z. (2016). Redefining the invertebrate RNA virosphere. *Nature*, *540*(7634), 539‑543. https://doi.org/10.1038/nature20167

Stentiford, G. D., Bonami, J.-R., & Alday-Sanz, V. (2009). A critical review of susceptibility of crustaceans to Taura syndrome, Yellowhead disease and White Spot Disease and implications of inclusion of these diseases in European legislation. *Aquaculture*, *291*(1), 1‑17. https://doi.org/10.1016/j.aquaculture.2009.02.042

Tamura, K., Stecher, G., & Kumar, S. (2021). MEGA11 : Molecular Evolutionary Genetics Analysis Version 11. *Molecular Biology and Evolution*, *38*(7), 3022‑3027. https://doi.org/10.1093/molbev/msab120

Ter Horst, S., Conceição-Neto, N., Neyts, J., & Rocha-Pereira, J. (2019). Structural and functional similarities in bunyaviruses : Perspectives for pan-bunya antivirals. *Reviews in Medical Virology*, *29*(3), e2039. https://doi.org/10.1002/rmv.2039

Valles, S. M., Chen, Y., Firth, A. E., Guérin, D. M. A., Hashimoto, Y., Herrero, S., De Miranda, J. R., Ryabov, E., & ICTV Report Consortium. (2017). ICTV Virus Taxonomy Profile : *Dicistroviridae*. *Journal of General Virology*, *98*(3), 355‑356. https://doi.org/10.1099/jgv.0.000756

Van Eynde, B., Christiaens, O., Delbare, D., Shi, C., Vanhulle, E., Yinda, C. K., Matthijnssens, J., & Smagghe, G. (2020). Exploration of the virome of the European brown shrimp (*Crangon crangon*). *Journal of General Virology*, *101*(6), 651‑666. https://doi.org/10.1099/jgv.0.001412

Veerassamy, S., Smith, A., & Tillier, E. R. M. (2003). A Transition Probability Model for Amino Acid Substitutions from Blocks. *Journal of Computational Biology*, *10*(6), 997‑1010. https://doi.org/10.1089/106652703322756195

Wang, J., Huang, Y., Xu, K., Zhang, X., Sun, H., Fan, L., & Yan, M. (2019). White spot syndrome virus (WSSV) infection impacts intestinal microbiota composition and function in *Litopenaeus vannamei*. *Fish & Shellfish Immunology*, *84*, 130‑137. https://doi.org/10.1016/j.fsi.2018.09.076

Wickham, H., Navarro, D., & Pedersen, T. L. (2016). *ggplot2 : Elegant Graphics for Data Analysis (3e)*. Springer-Verlag New York.

Figure captions

Fig. 1 Graphical representation of the segmented (-) ssRNA genome of Astacus bunya-like virus 1 with read coverage plot (reads mapped back to the genome sequence; red curve) and schematic terminal decamer sequences (insets). The 5' terminus of each segment (L, M, S) consists of the conserved decamer …CAGUAACACA and the 3' terminus of the reverse complement UGUGUNNCUG…, where NN are two nucleotides which differ between the three segments (CA, UA, UU, respectively). This reverse complementarity permits non-covalent bonding of both termini, rendering the genome segments pseudo-circular. Note that the 3' terminus could not be confirmed for segment M (probable sequence is indicated here in transparency).

Fig. 2 Phylogenetic comparison of the RNA-dependent RNA polymerase protein sequence of Astacus bunya-like virus 1 and representative members of the *Phenuiviridae*, rooted with a member of the *Peribunyaviridae* (*Peribun.*) and the crayfish-infecting athtab bunya-like virus as outgroup. Note that the phylogenetical position of athtab bunya-like virus is unclear. Selection of sequences is inspired by Grandjean et al. (2019). Sequences were aligned using MAFFT (v. 7.475; Katoh & Standley, 2013) and the tree was built with the maximum likelihood method and the LG+F+R4 model (Le & Gascuel, 2008), with 1000 bootstrap replicates. Numbers on the nodes represent bootstrap percentages. Scale bar corresponds to estimated amino acid substitutions per site.

Fig. 3 Genome structure of Astacus hepe-like virus 1-4 compared to the closely related signal crayfish associated hepe-like virus 1 (OK317707). The four viruses have a genome organised into five open reading frames (ORFs). The fifth ORF is not described in the reference sequence (OK317707), but can be predicted by an ORF finder, and is shown here in transparency. The

ORF 1-encoded polyprotein contains methyltransferase (MeT) and helicase (Hel) domains, and the ORF 2-encoded hypothetical protein 1 (HP1) an RNA-dependent RNA polymerase (RdRp) domain. The amino acid identity percentage between each virus and the reference is annotated for each ORF and predicted domain.

Fig. 4 Phylogenetic comparison of the RNA-dependent RNA polymerase protein sequence of Astacus hepe-like virus 1-4 with a selection of blastx hits and representative members of the *Hepeviridae*. Icons next to sequence names represent the animal from which the viruses were described. Sequences were aligned using MAFFT (v. 7.475; Katoh & Standley, 2013) and a midpoint-rooted tree was built with the maximum likelihood method and the Blosum62+F+R3 model (Henikoff & Henikoff, 1992), with 1000 bootstrap replicates. Numbers on the nodes represent bootstrap percentages. Scale bar corresponds to estimated amino acid substitutions per site.

Supplementary material captions

Fig. S1 Geographical repartition of seven noble crayfish (*Astacus astacus*) populations sampled for RNA virome analysis in Switzerland. Populations originated from four Swiss cantons (Aargau (AG1), St. Gallen (SG1-4), Solothurn (SO1) and Thurgau (TG1)). Crayfish in populations SO1 and TG1 experienced mortality.

Table S1 Table containing information on sequences similar to fungi-infecting viruses (*Narnaviridae, Mitoviridae, Totiviridae*). The table (sorted per population) contains the sequence, length and k-mer coverage (kmercov), the best-hit in blastx analysis (blastx_besthit) with associated identity percentage (blastx_identity) and alignment length in amino acids (blastx_lengthalignment) between the sequence and its best-hit.

Primer name	Sequence (5'-3')
LF1_3'RACE	AGGAGATCCCCTGCTAGGTC
LF2_3'RACE	ACTGCTGAATTGGTGCCCAT
LR1_5'RACE	AGCTGATACCTCTCTTTGCCT
LR2_5'RACE	TCCAATGGCTCAATGGTGAA
MF1_3'RACE	GGCTGGCAGTTAGTCCTGTT
MF2_3'RACE	ATTGCAGTGGGTCTGGACAG
MR1_5'RACE	GACTTCCTCCCCCTGGTTTG
MR2_5'RACE	CCACTCCACTTCCCACCATC
SF1_3'RACE	CCTACTGAACTCAAGGCATT
SF2_3'RACE	GAATATGAAGACTGCAGCCT
SR1_5'RACE	TCTTTGGGGTTTATCTGCTC
SR2_5'RACE	TCTCCCCTCTTTTCTCTAGG
LF_RT	AGTGATGGAGGCAATGTGGG
LR_RT	TTTGCAACATGGTGCCCTTG
MF_RT	ATTGCAGTGGGTCTGGACAG
MR_RT	AACATGAGGACAACCCACCC
SF_RT	TGGGAGCGGAATCCTACTGA
SR_RT	GGCCTTCTCCTTCCTGGTTC
Aplv2_F	TTCCAACTGTGCCTCGAGTC
Aplv2_R	AGAACCAGTACGCTTTCGCA

Table S2 List of primers used for Rapid amplification of cDNA ends (RACE)-PCR and one-step RT-PCR.

Fig. S2 Geneious alignments of Astacus bunya-like virus 1 L, M and S segments with the corresponding deposited sequences of bunya-like brown spot virus (MK881590, MK881591, MK881592, respectively). Yellow boxes represent the coding sequences (CDS) of each segment, and white boxes the untranslated regions.

Fig. S3 Phylogenetic comparison of the glycoprotein sequence of Astacus bunya-like virus 1 with representative members of the *Phenuiviridae* and bunyamwera virus (*Peribunyaviridae*) as outgroup. Sequences were aligned using MAFFT (v. 7.475; Katoh & Standley, 2013) and the tree was built with the maximum likelihood method and the PMB+F+R3 model

(Veerassamy et al., 2003), with 1000 bootstrap replicates. Numbers on the nodes represent bootstrap percentages. Scale bar corresponds to estimated amino acid substitutions per site.

Fig. S4 Phylogenetic comparison of the nucleocapsid protein sequence of Astacus bunya-like virus 1 with representative members of the *Phenuiviridae* and bunyamwera virus (*Peribunyaviridae*) as outgroup. Sequences were aligned using MAFFT (v. 7.475; Katoh & Standley, 2013) and the tree was built with the maximum likelihood method and LG+G4 model (Le & Gascuel, 2008), with 1000 bootstrap replicates. Numbers on the nodes represent bootstrap percentages. Scale bar corresponds to estimated amino acid substitutions per site.

Figure S5. Percentage of pairwise amino acid identity between each Astacus hepe-like virus for each of the five open reading frames (ORF).

Graphical Abstract

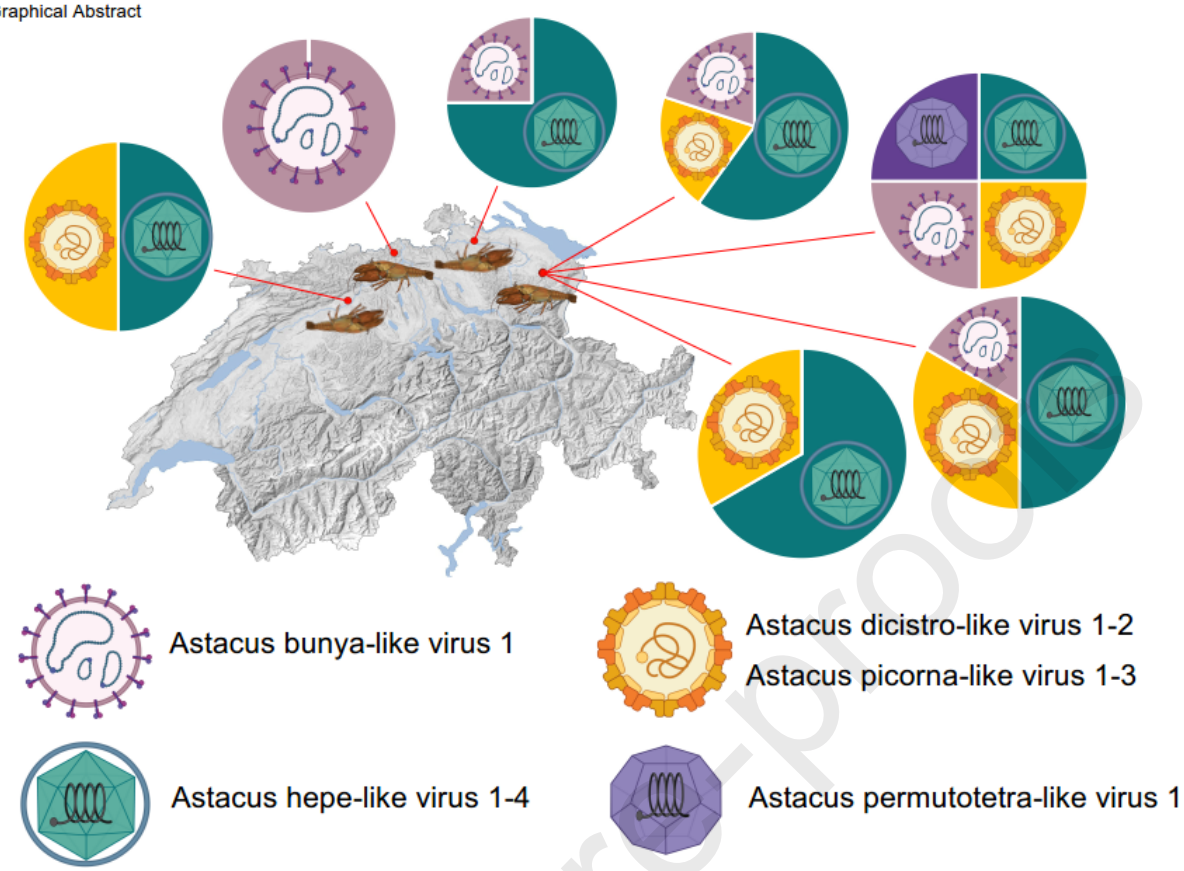

Declaration of interests

☒ The authors declare that they have no known competing financial interests or personal relationships that could have appeared to influence the work reported in this paper.

☐ The authors declare the following financial interests/personal relationships which may be considered as potential competing interests:

Figure 1

Click here to access/download;Figure;Fig. 1.pdf

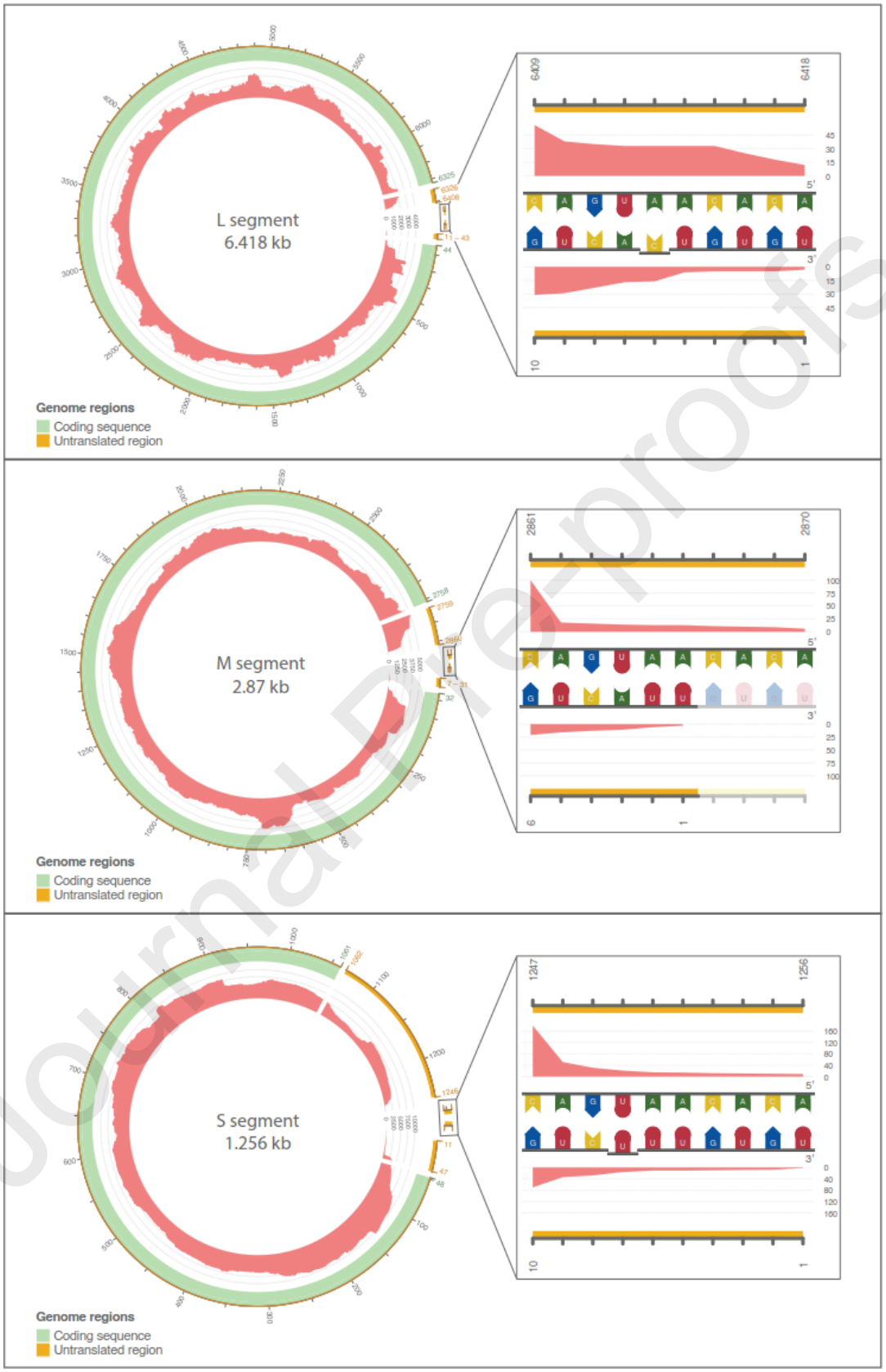

Figure 2

Click here to access/download;Figure;Fig. 2.pdf

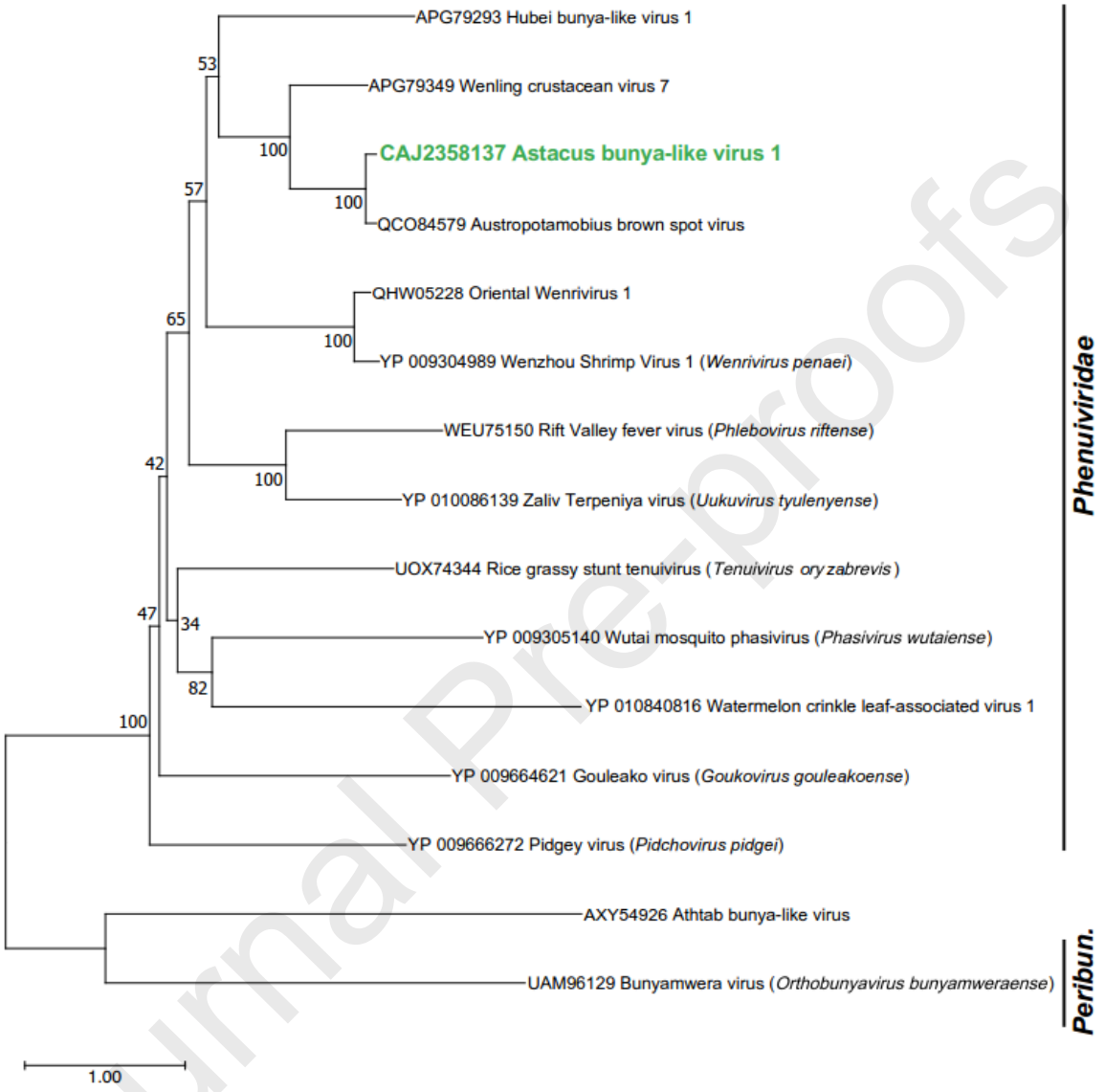

Figure 3

Click here to access/download;Figure;Fig. 3.pdf

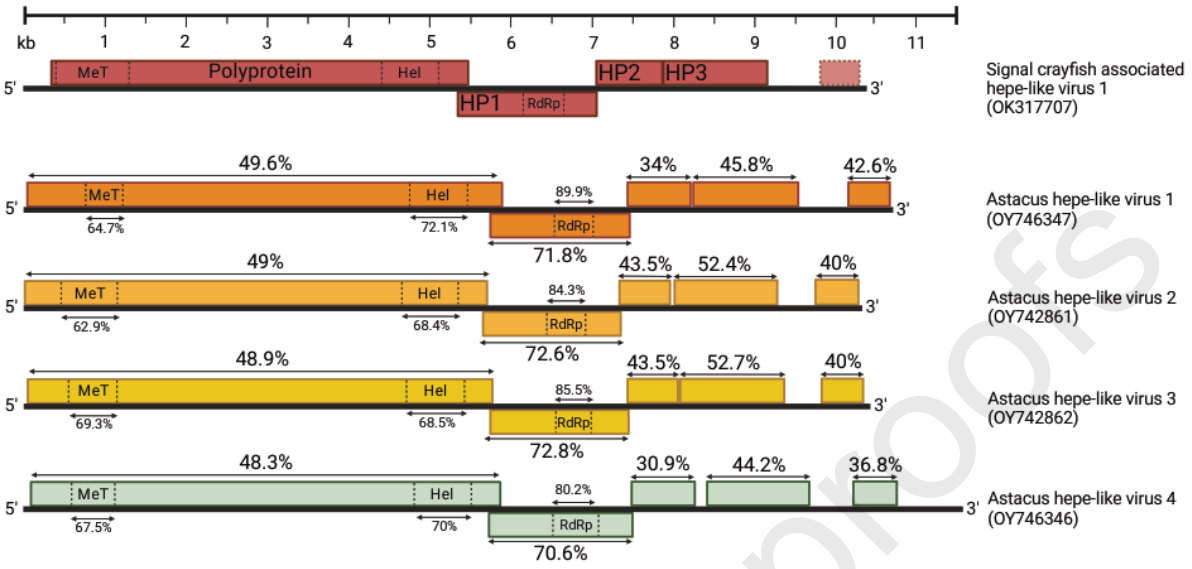

Figure 4

Click here to access/download;Figure;Fig. 4.pdf